Journal of Microbiology (2014) Vol. 52, No. 8, pp. 667–674
DOI 10.1007/s12275-014-4113-1

Evaluation of the Antimicrobial Potency of Silver Nanoparticles Biosynthesized by Using an Endophytic Fungus, *Cryptosporiopsis ericae* PS4

Lamabam Sophiya Devi and Santa Ram Joshi*

Microbiology Laboratory, Department of Biotechnology and Bioinformatics, North-Eastern Hill University, Shillong 793022, India

(Received Feb 21, 2014 / Revised Apr 17, 2014 / Accepted Apr 21, 2014)

In the present study, silver nanoparticles (AgNPs) with an average particle size of 5.5 ± 3.1 nm were biosynthesized using an endophytic fungus *Cryptosporiopsis ericae* PS4 isolated from the ethno-medicinal plant *Potentilla fulgens* L. The nanoparticles were characterized using UV-visible spectrophotometer, transmission electron microscopy (TEM), scanning electron microscopy (SEM), selective area electron diffraction (SAED), and energy dispersive X-ray (EDX) spectroscopy analysis. Antimicrobial efficacy of the AgNPs was analyzed singly and in combination with the antibiotic/antifungal agent chloramphenicol/fluconazole, against five pathogenic microorganisms-*Staphylococcus aureus* MTCC96, *Salmonella enteric* MTCC735, *Escherichia coli* MTCC730, *Enterococcus faecalis* MTCC2729, and *Candida albicans* MTCC 183. The activity of AgNPs on the growth and morphology of the microorganisms was studied in solid and liquid growth media employing various susceptibility assays. These studies demonstrated that concentrations of AgNPs alone between 10 and 25 μM reduced the growth rates of the tested bacteria and fungus and revealed bactericidal/fungicidal activity of the AgNPs by delaying the exponential and stationary phases. Examination using SEM showed pits and ruptures in bacterial cells indicating fragmented cell membrane and severe cell damage in those cultures treated with AgNPs. These experimental findings suggest that the biosynthesized AgNPs may be a potential antimicrobial agent.

Keywords: silver nanoparticles, biosynthesis, endophyte, *Cryptosporiopsis ericae*, antimicrobial

Introduction

The emergence of bacterial resistance to antibacterial drugs has become a major problem in public health due to the uncontrolled use and abuse of conventional antibiotics. Antimicrobial resistance results from an evolutionary processes taking place during antibiotic therapy, such that resistant bacteria survive the treatment and pass this trait to their progeny. Horizontal gene transfer by conjugation, transduction, or transformation constitutes other mechanisms used by the bacteria to transfer this resistance. This has prompted the development of alternative strategies to treat bacterial diseases. Metal nanoparticles have emerged as novel antimicrobial agents. Several classes of antimicrobial nanoparticles and nanosized carriers for antibiotics delivery have proven to be effective *in vitro* and in infectious disease animal models, including those using antibiotic-resistant bacteria (Huh and Kwon, 2011). Nanoparticles are clusters of atoms in the size range of 1–100 nm. The word "nano" is derived from Greek meaning extremely small. The use of nanoparticles is gaining impetus in the present century because they possess defined chemical, optical, and mechanical properties. Metallic nanoparticles are the most promising because they show good antimicrobial properties owing to their large surface area to volume ratio (Gong *et al*., 2007). Among the noble metals, silver is preferred because it has been known since ancient times to be an effective antimicrobial agent for the treatment of diseases, for food preservation and to keep water potable. With the recent advancements in the field of nanotechnology, AgNPs have been widely used as a novel therapeutic agent extending their use as antibacterial, antifungal, antiviral, anti-inflammatory, and anti-cancerous agents (Vaidyanathan *et al*., 2009).

To date, the conventional approaches used for nanoparticles synthesis include reduction of metals in solutions (Goia and Matijevie, 1998), chemical and photochemical reactions in reverse micelles (Taleb *et al*., 1997), thermal decomposition of silver compounds (Esumi *et al*., 1990), and electrochemical (Rodriquez-Sanchez *et al*., 2000), sonochemical (Zhu *et al*., 2000), radiation-assisted (Henglein, 2001), and microwave-assisted processes (Pastoriza-Santos and Liz-Marzan, 2002). However, these methods have certain disadvantages owing to the involvement of toxic chemicals and radiation. Many of the reducing agents, solvents, and additives used in the reduction process pose severe environmental and biological risks. This has prompted the development of eco-friendly and simple processes, especially for the large-scale production of these materials. The importance of developing eco-friendly synthesis methods of nanoparticles has been recognized, and several attempts of green chemistry route for synthesis of metal nanoparticles have been made (Bar *et al*., 2009; Begum *et al*., 2009; Song and Kim, 2009; Malabadi *et al*., 2012; Nalwade *et al*., 2013). Microorganisms such as bacteria, yeast, and fungi play an important role in remediation of toxic metals through re-

*For correspondence. E-mail: srjoshi2006@yahoo.co.in; Tel.: +919436102171; Fax: +913642550076

duction of metal ions, and they are considered interesting as potential nanofactories (Fortin and Beveridge, 2000). Therefore, they are candidates for the development of more environmentally friendly manufacturing techniques that may avoid hot, high-pressure, and caustic processes. Filamentous fungi are ideal candidates for the synthesis of metal nanoparticles because the fungi are easy to handle and cultivate on a large scale (Mukherjee *et al.*, 2001). Fungi can accumulate metals by physicochemical and biological mechanisms including extracellular binding by metabolites and polymers, binding to specific polypeptides, and metabolism dependent accumulation.

Many earlier studies have demonstrated the mycosynthesis of AgNPs (Ahmad *et al.*, 2003; Bhainsa and d'Souza, 2006; Gade *et al.*, 2008; Gade *et al.*, 2010; Devi and Joshi, 2012). The mycosynthesis of metal nanoparticles, or myconanotechnology (Rai *et al.*, 2009), is at the interface between mycology and nanotechnology. Endophytes are the chemical synthesizers inside plants (Owen and Hundley, 2004) and provide a broad variety of bioactive secondary metabolites with unique structures, including alkaloids, benzopyranones, flavonoids, phenolic acids, quinones, and antibiotics (Tan and Zou, 2001; Bhagobaty and Joshi, 2011). Various attempts have been made to isolate and identify various bioactive metabolites from endophytic fungi (Strobel, 2003; Strobel and Daisy, 2003). However, few studies have investigated the biosynthesis of AgNPs using endophytic fungi (Verma *et al.*, 2010; Devi *et al.*, 2013; Qian *et al.*, 2013).

The present study was conducted to examine the potential eco-friendly biosynthesis of biologically active AgNPs using the endophytic fungus *Cryptosporiopsis ericae* PS4, which was isolated from an ethno-medicinal plant *Potentilla fulgens* L. To our knowledge, the use of *C. ericae* for biosynthesizing nanoparticles has not been previously reported.

Materials and Methods

Isolation and characterization of endophytic fungus

The endophytic fungus was isolated according to the method described by Strobel *et al.* (1996) with minor modifications. Genomic DNA of the fungal endophyte was extracted using a genomic DNA miniprep purification spin kit (Qiagen, Germany). Internal transcribed spacer (ITS) regions (ITS1, 5.8S and ITS2) were amplified using primers ITS1 5′-TCC GTAGGTGAACCTGCGG-3′ and ITS4 5′-TCCTCCGCTT ATTGATATGC-3′ (White *et al.*, 1990) using a 9700 Gold thermal cycler (Applied Biosystems, UK) under the following conditions: initial denaturation at 94°C for 1 min, annealing temperature at 52°C for 1 min and extension at 72°C for 1 min with an initial denaturation and final extension for 5 and 10 min at 94 and 72°C, respectively (Musarrat *et al.*, 2010). The amplified PCR products were purified using QIA quick gel extraction kit (Qiagen), which were subsequently sequenced using BigDye terminator (Applied Biosystems). The resulting sequences were analyzed using the BLAST algorithm of National Centre of Biological Information (NCBI) database to obtain closely related phylogenetic sequences. The phylogenetic tree was constructed using neighbor-joining method with the MEGA5 software.

Extracellular biosynthesis of AgNPs

The fungal biomass was prepared by aerobic culture in potato dextrose broth containing an infusion of 250 g potato and 20 g dextrose/L of distilled sterile water. The inoculated flasks were incubated on an orbital shaker at 25 ± 2°C and agitated at 120 rpm for 96 h. The biomass was harvested by filtering, followed by repeated washing with distilled sterile water. Ten gram (wet weight) of the biomass was added to 100 ml of sterilized double distilled water, followed by incubation for 48 h at 25 ± 2°C in a shaker at 120 rpm. Then, the biomass was filtered through Whatman filter paper No. 1. The filtrate thus obtained was treated with a 1 mM silver nitrate (Sigma Aldrich) solution in an Erlenmeyer flask and incubated at room temperature in the dark. Control filtrates without silver nitrate solution were also incubated.

Characterization of biosynthesized AgNPs

The bioreduction of precursor silver ions was monitored by periodically analyzing the sample using UV-visible spectroscopy. Absorption measurements were carried out on UV-visible spectrophotometer (CARY-100 BIO UV-Vis Spectrophotometer; Varian Inc., USA) at a resolution of 1 nm, and in the range of 200–800 nm ranges. Morphological analyses of the AgNPs were carried out using SEM and TEM analysis, as follows. Biosynthesized AgNPs was drop cast on carbon coated copper grids and dried under vacuum desiccation and TEM micrographs of the sample were taken using the JEOL JSM 100CX TEM instrument (Jeol, Japan) operated at an accelerating voltage of 200 kV. Average silver core diameter (D), size distributions, and standard deviations were calculated for each nanoparticle sample by averaging 200 particles from the TEM images using ImageJ software (developed at the National Institutes of Health). The presence of elemental silver was confirmed through EDX spectroscopy. In order to carry out SEM and EDX analysis, AgNPs solution was centrifuged for 20 min at 10,000 rpm and drop coated on to thin glass film. SEM and EDX analysis was then performed using SEM, Leo 1430vp microscope equipped with an EDAX attachment (Carl Zeiss, Germany).

Determination of AgNPs concentration

The concentration of AgNPs was determined by the method of Liu *et al.* (2007).

To determine the average number of atoms per nanoparticle, the following relation was used:

$$N = \frac{\pi \rho D^3}{6M} N_A$$

Where, N is the number of atoms per nanoparticles, π= 3.14, ρ is the density of face centered, cubic (fcc) silver (10.5 g/cm^3), D is the average diameter of nanoparticles, M is the atomic mass of silver (107.868 g), NA is the number of atoms per mole (Avogadro's number = 6.023 × 1023).

The molar concentration of the nanoparticle solution was determined using the following formula:

$$C = \frac{N_T}{NVN_A}$$

Where, C is the molar concentration of nanoparticle solution, N_T is the total number of silver atoms added as $AgNO_3$ =1 M, N is the number of atoms per nanoparticle, V is the volume of the reaction solution in L, N_A is the Avogadro's number.

Antimicrobial analysis

The antimicrobial activity of the synthesized AgNPs was assessed against the following Gram-positive and -negative pathogenic bacteria, *Staphylococcus aureus* MTCC96, *Salmonella enterica* MTCC735, *Escherichia coli* MTCC730, and *Enterococcus faecalis* MTCC2729 plus also the pathogenic fungus *Candida albicans* MTCC183. The assays were performed by plating the individual test organism on Mueller Hinton agar (MHA) medium. Wells were cut in the plates using a sterile cork-borer and 50 µl of AgNPs solution was dispensed in each well. The mycelia-free water extract alone was used as control. The plates were incubated overnight at 37°C and observed for of zones of inhibition.

The combined effect of extracellularly synthesized AgNPs with the commonly used broad spectrum antimicrobial agents Chloramphenicol/Fluconazole (HiMedia, India) was studied against the five test microorganisms. To determine the synergistic effect, an antibiotic disk alone or a disk impregnated with 20 µl of freshly prepared AgNPs was placed onto the Muller-Hinton agar (MHA) medium inoculated with test organisms. Fungal cell-free filtrate was used as a negative control. After incubating at 25°C for 24–48 h the plates were observed for the antimicrobial activity (Zones of growth inhibition) of the antibiotic alone and in combination with AgNPs. All the assays were performed in triplicate. The increase in fold area was assessed by calculating the mean surface area of the inhibition zone generated by the antibiotic alone and in combination with AgNPs or the negative control. The fold area increase was calculated by the equation $(b^2 - a^2)/a^2$, where "a" and "b" refer to the zones of inhibition for antibiotic alone and antibiotic with AgNPs respectively (Birla *et al.,* 2009).

Further, minimum inhibitory concentration (MIC) of biosynthesized AgNPs was also measured (Mayr-Harting *et al.*, 1972). Bacterial inoculum of *S. aureus* MTCC96, *S. enterica* MTCC735, *E. coli* MTCC730, and *E. faecalis* MTCC2729 as well as the fungal inoculum of *C. albicans* MTCC183 were prepared by growing a single colony overnight in nutrient broth (NB)/Potato dextrose broth (PDB) and adjusting the turbidity to 0.5 McFarland standards. The NB/PDB media was supplemented with different concentrations of nanoparticles (1, 5, 10, 15, 20, and 25 µM) and inoculated with bacterial suspension. Control tubes were maintained without AgNPs. The MIC was determined after 24 h of incubation at 37°C by observing the visible turbidity and measuring the optical density of these culture broths at 600 nm (Panacek *et al.*, 2006). The MBC was also determined by plating the treated cells on agar plates.

In order to elucidate the antibacterial mechanism of AgNPs, SEM and TEM techniques were used. Cells of test strains before and after treatment with nanoparticles were fixed overnight with 2.5% glutaraldehyde and drop coated on silicon wafers. Air-dried samples were sputter coated with gold and observed under SEM.

Growth kinetics in the presence of AgNPs

To study the bacterial growth kinetics in the presence of AgNPs, bacteria and fungus were grown in 100 ml of NB/PDB medium. Growth was allowed until the optical density reached 0.1 at 600 nm (OD of 0.1 corresponds to a concentration of 10^8 CFU/ml of medium). Subsequently, 2×10^8 CFU from above were inoculated into 100 ml liquid NB/PDB media supplemented with different concentrations of AgNPs (1, 5, 10, 15 µM). Control broths were used without nanoparticles. The plate was incubated at 37°C and 100 rpm and growth rate was determined by recording the absorbance at 600 nm for 30 h at regular time interval.

Results and Discussion

Identification of Fungal isolate

The ITS sequence obtained was deposited in the NCBI GenBank (accession no. JX853765). Based on the sequence of the

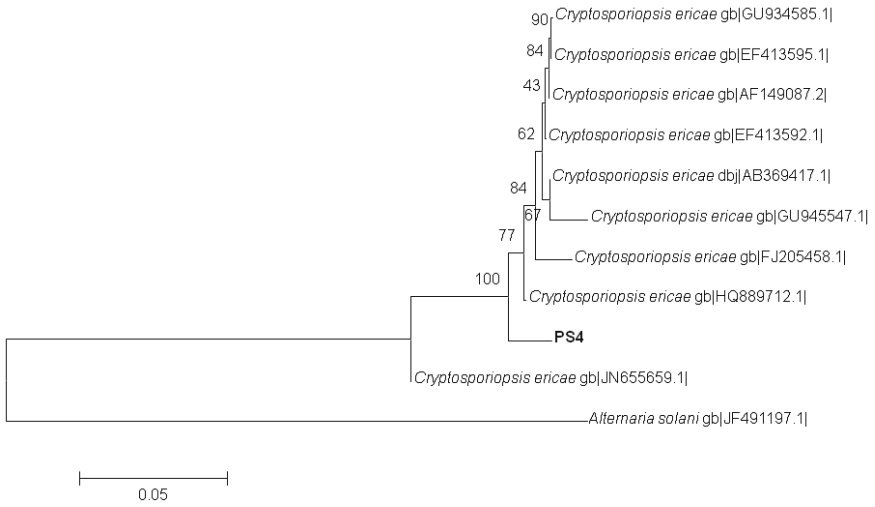

Fig. 1. Phylogenetic relationship between the isolate *C. ericae* PS4 and other closely related reference microorganisms retrieved from NCBI GenBank.

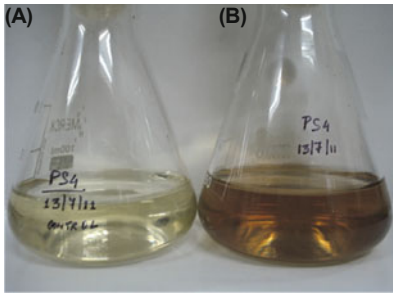

Fig. 2. Erlenmeyer flask containing cell-free filtrate of *C. ericae* PS4 without (A) and with (B) silver nitrate solution (1 mM) after 72 h of reaction.

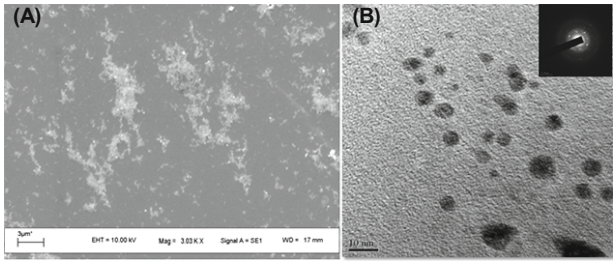

Fig. 4. (A) SEM micrograph of biosynthesized AgNP, (B) TEM micrograph of biosynthesized AgNPs [Inset: SAED pattern of the AgNPs].

ITS region of its rRNA genes, the fungal endophyte isolated from *Potentilla fulgens* L. was identified as *C. ericae* PS4 based on the ITS sequence BLAST searches, which shared 98% identity with *C. ericae* (HQ889712). The closest homologues to the sequences were selected and multiple sequence alignments were carried out using the ClustalW program in the MEGA5 software. A phylogenetic tree was constructed using the neighbor-joining algorithm with 1,000 bootstrap replications (Fig. 1).

Biosynthesis and characterization of AgNPs

After treating the cell free filtrate of *C. ericae* PS4 with 1 mM $AgNO_3$, the solution changed from pale yellow to brown, while no color change was observed in the control (Figs. 2A and 2B). The appearance of a brown color in the solution indicates the formation of AgNPs in the reaction mixture. Prior studies by Wiley and colleagues showed that AgNPs produce a brown solution in water, due to the surface plasmon resonances (SPR) effect, which indicates the transition of $AgNO_3$ to AgNPs (Wiley *et al.*, 2006). The UV-visible spectra of the cell-free filtrate and the filtrate treated with 1 mM $AgNO_3$ at different time intervals is presented in Fig. 3. UV-visible spectrophotometer analysis of the cell filtrate without $AgNO_3$ showed an absorption peak at 280 nm, which corresponds to aromatic amino acids of proteins (Fig. 3). The peak at 280 nm can be attributed to the tryptophan and tyrosine residues present in proteins (Bhainsa and D'Souza, 2006). This observation indicates the presence of proteins secreted by fungus in the cell-free filtrate. The UV-visible spectrophotometer analysis of the cell filtrate with $AgNO_3$ showed the absorbance at around 440 nm in the form of a sharp peak in addition to the absorption peak at 280 nm, which is specific for the synthesis of AgNPs. We found a correlation with the time of incubation; the longer the incubation time, the greater the absorption at 440 nm. This is indicative of relatively small and spherical silver particles, which attained maximum intensity on the third day (72 h) (Fig. 3). These findings corroborate with the report by Dar *et al.* (2012), in which AgNPs synthesized by *Cryphonectria* spp. showed an absorption peak at approximately 440 nm due to excitation owing to the SPR effect.

Measurements using SEM and TEM were used to determine the morphology of the synthesized nanoparticles. Images and measurements based on SEM, showed that the AgNPs morphology was approximately spherical (Fig. 4A). Transmission electron micrographs confirmed the spherical shape and uniformly distribution without significant agglomeration. The analysis of data obtained from TEM micrographs of AgNPs showed that the particle size ranged from 2 to 15 nm, with an average size of 5.5 ± 3.1 nm (Fig. 4B). The particle size histogram of the AgNPs is shown in Fig. 5. The SAED pattern reveals the crystalline nature of the biosynthesized nanoparticles (Fig. 4 Inset: SAED pattern of the AgNPs). In the analysis by energy dispersive X-ray spectroscopy of the

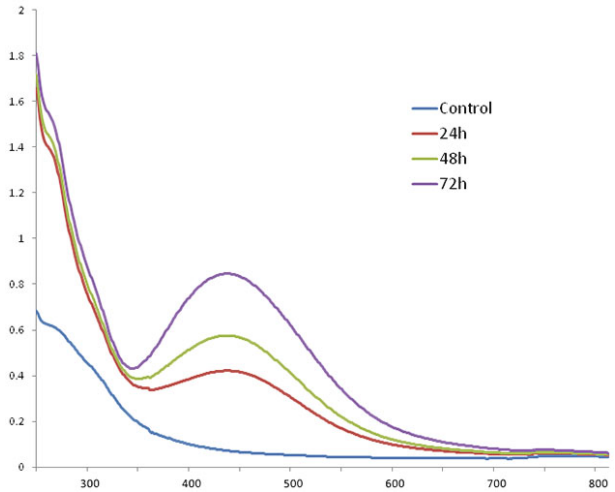

Fig. 3. The UV-Visible absorption spectra of extracellularly synthesized AgNPs.

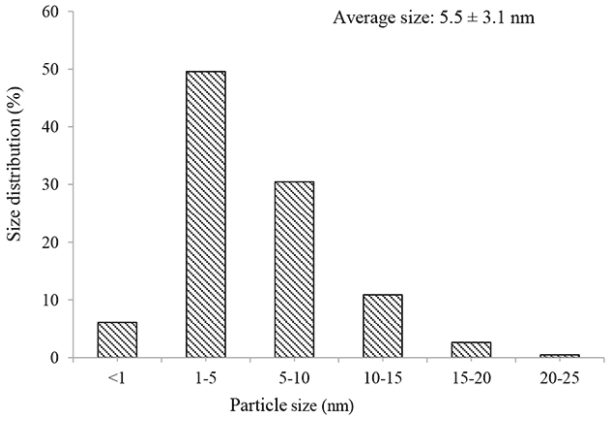

Fig. 5. Particle size distribution pattern histogram of the biosynthesized AgNPs.

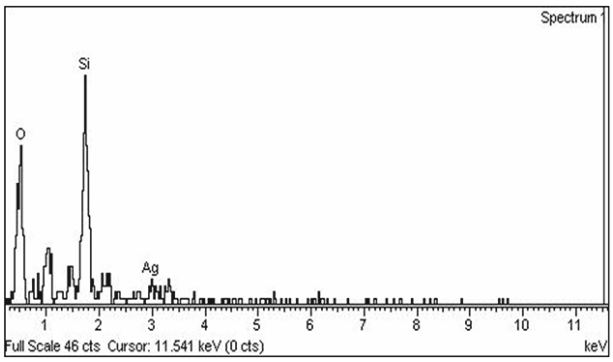

Fig. 6. **EDX spectra of the biosynthesized AgNPs.**

AgNPs, the presence of an elemental metal signal was confirmed. The EDX profile shows the presence of a characteristic silver signal at approximately 3 keV (Fig. 6), which is typical for the absorption of AgNPs due to surface plasmon resonance. These data together demonstrate successful AgNPs biosynthesis using an endophytic fungal extract.

Antimicrobial study

Smaller particles with a larger surface area possess higher antibacterial effects compared to larger particles (Panacek *et al*., 2006). Gram-negative and Gram-positive bacteria including antibiotic-resistant strains are targeted by AgNPs, which to date have not shown to result in bacterial resistance. The antimicrobial efficacy of the biosynthesized AgNPs was assessed against various pathogens. The results showed that AgNPs possess antimicrobial activity against the tested pathogens (Table 1), which included Gram-negative and -positive bacteria plus the pathogenic fungus *C. albicans*. Because the biosynthesized AgNPs produced by *C. ericae* PS4 showed considerable antibacterial and antifungal activity, they could have potential clinical and biomedical applications as antimicrobial agents. The synergy of the antibiotic/antifungal agent with AgNPs was also investigated. The diameter of inhibition zones and increase in fold area for all the test bacteria and fungus was measured (Table 1). The antibacterial activity of the broad-spectrum antibiotic chloramphenicol against the tested strains increased significantly in presence of AgNPs and also the antifungal activity of antifungal agent fluconazole was also found to increase when combined with the biosynthesized AgNPs. Therefore, such AgNPs could be potentially used as antimicrobial agent alone or in combination with antibiotics, but this still requires further investigation.

The MIC and MBC of the AgNPs were found to be 15 µM and 20 µM respectively for the Gram-negative bacterial strains *E. coli* MTCC730 and *S. enterica* MTCC735 (Figs. 7A and 7B). For the Gram-positive strains *S. aureus* MTCC96 and *E. faecalis* MTCC2729, MIC, and MBC were 20 µM

Table 1. **Mean zone of inhibition (mm) of biosynthesized AgNPs singly or in combination with chloramphenicol/fluconazole against the test organisms as compared to activity of fungal cell free extract**

Test microorganisms		Zone of inhibition (mm) (mean of three replicates)				
		AgNPs	Chloramphenicol/fluconazole	AgNPs + Chloramphenicol/fluconazole	Increase in fold area	Cell free filtrate (control)
Bacteria	*S. enterica* MTCC735	15±0.5	32	37	0.34	-
	E. coli MTCC730	17±0.5	28	35	0.56	-
	S. aureus MTCC96	14±1.0	32	36	0.44	-
	E. faecalis MTCC2729	14±0.5	30	38	0.41	-
Fungus	*C. albicans* MTCC183	19±0.5	31	35	0.27	-

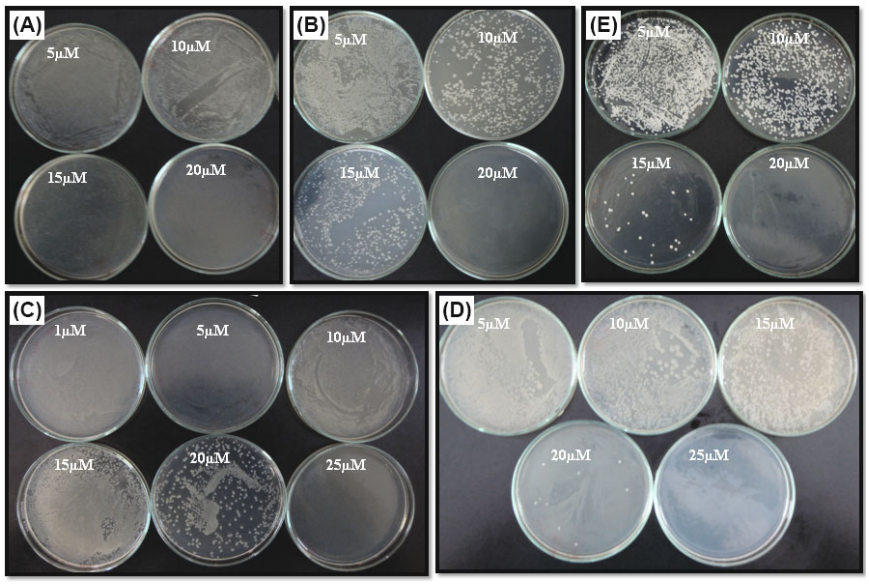

Fig. 7. **MBC of the biosynthesized AgNPs against (A) *E. coli* MTCC730, (B) *S. enterica* MTCC735, (C) *S. aureus* MTCC96, (D) *E. faecalis* MTCC2729, and (E) *C. albicans* MTCC183.**

and 25 µM, respectively (Figs. 7C and 7D). In the case of *C. albicans* MTCC183, the MIC was obtained at a lower concentration of 10 µl (Fig. 7E). The minimal antimicrobial activity of AgNPs was greater for Gram-positive bacteria compared to Gram-negative bacteria. This is due to the high lipopolysaccharide and thick peptidoglycan layer of the Gram-positive microorganisms, which results in minimal binding sites for AgNPs (Fayaz *et al.*, 2010). The mechanism by which the nanoparticles are able to inhibit bacterial growth is not well understood, but it is suggested that the silver nanoparticles affects the bacterial membrane. The interaction of AgNPs with the bacterial membrane may lead to significant increases in the permeability and affect membrane transport (Sondi and Salopek-Sondi, 2004). The silver nanoparticles also penetrate inside the bacteria and can disturb the functions of sulfur-containing proteins and phosphorus-containing DNA and proteins, leading to the inhibition of enzyme functions (Singh *et al.*, 2008; Gordon *et al.*, 2010). Further studies are required to determine the mechanisms by which biosynthesized AgNPs produced by *C. ericae* PS4 exert their antibacterial and antifungal activity.

Growth curves of the cultures treated with AgNPs indicated inhibition of the growth and reproduction of bacteria and fungi by AgNPs. Increasing concentrations of AgNPs significantly delayed the exponential phase as compared to untreated samples and led to complete arrest of growth (Figs. 8A–8E). The lowest concentration of AgNPs, which eliminated the growth of all bacterial strains tested, was observed at 15 µM concentration (Figs. 8A–8D). However, complete inhibition in the growth of *C. albicans* MTCC183 was found at a concentration of 10 µM AgNPs (Fig. 8E).

The effect of AgNPs on the morphology of the bacterial

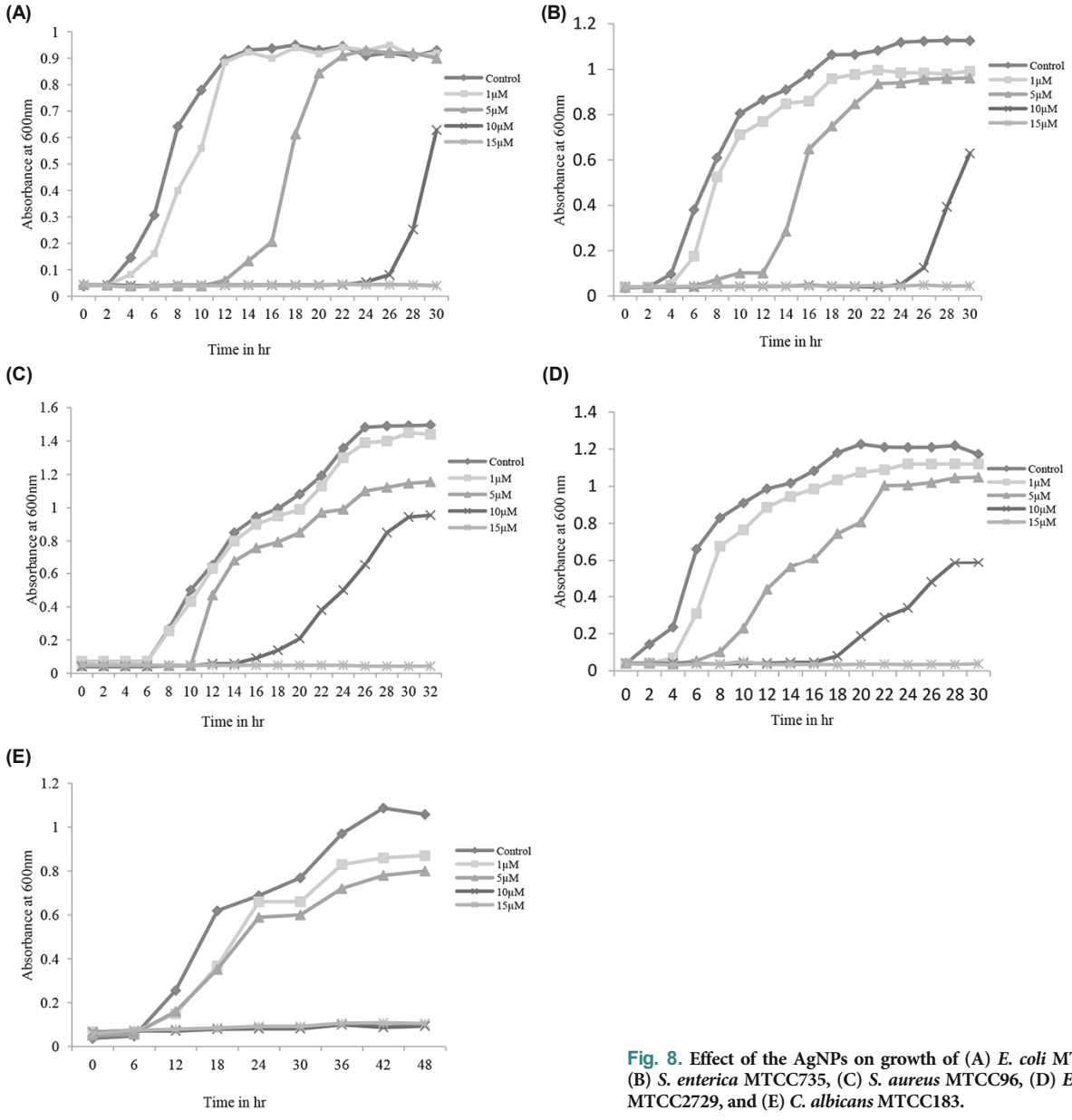

Fig. 8. Effect of the AgNPs on growth of (A) *E. coli* MTCC730, (B) *S. enterica* MTCC735, (C) *S. aureus* MTCC96, (D) *E. faecalis* MTCC2729, and (E) *C. albicans* MTCC183.

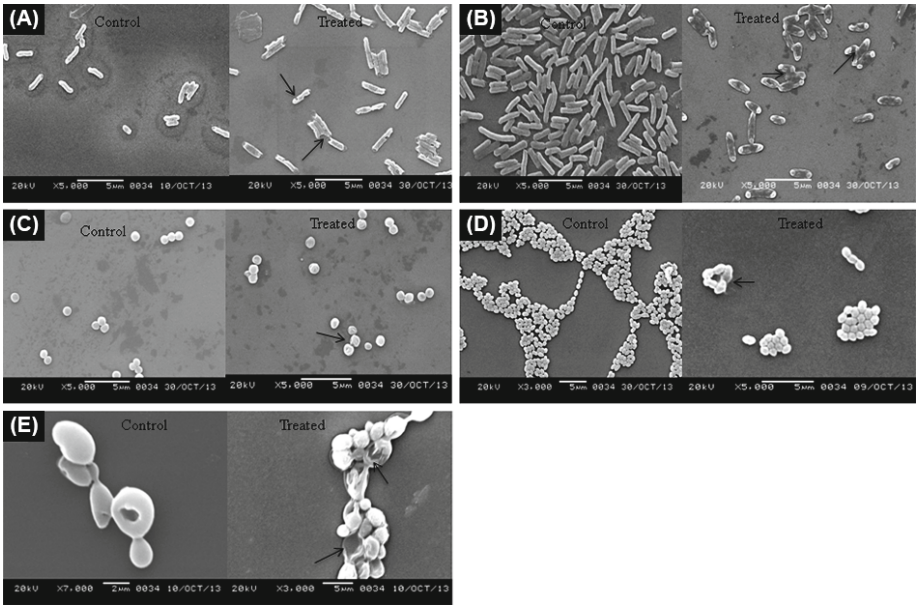

Fig. 9. **Scanning electron micrograph of cells of (A) *S. enterica* MTCC735, (B) *E. coli* MTCC730, (C) *S. aureus* MTCC96, (D) *E. faecalis* MTCC2729, and (E) *C. albicans* MTCC183 without and with AgNPs treatment (Arrows indicate the cell wall rupture/breakage).**

and fungal cells was evaluated using SEM. The cell surface of untreated cells was intact and damage was not seen. However, after treatment with nanoparticles, structural changes and major damage in the morphology of cells was clearly observed in the scanning electron micrographs (Figs. 9A–9E). In case of the Gram-negative bacteria *E. coli* MTCC730 and *S. enterica* MTCC735, very clear deformation and fragmentation of the cell membrane was observed. The morphological membrane disruption of Gram-positive bacteria *S. aureus* MTCC96 and *E. faecalis* MTCC2729 was much lesser compared to Gram-negative bacteria *E. coli* MTCC730 and *S. enterica* MTCC735. This difference could be attributed to the difference of the peptidoglycan layer of the bacterial cell between Gram-positive and Gram-negative bacteria. SEM analysis also revealed the ability of silver nanoparticles to disrupt the fungal envelope structure. The result showed that the treated fungal cells of *C. albicans* MTCC183 showed significant damage, which was characterized by the rupture of cell membrane. These observations supports the earlier findings on the antibacterial mechanism of AgNPs (Sondi and Salopek-Sondi, 2004; Cho *et al.*, 2005; Kim *et al.*, 2011; Kora and Arunachalam, 2011).

Conclusion

To our knowledge, the present study is the first report on the synthesis of AgNPs using the endophytic fungus *Cryptosporiopsis ericae* PS4 isolated from the medicinal plant *Potentilla fulgens* L. The biosynthesized AgNPs could efficiently inhibit various pathogenic organisms, including four bacterial and a fungal species. The potential anti-microbial AgNPs biosynthesized by the endophytic fungus offers promising scope for their eco-friendly and sustainable production using microbial cell factories.

Acknowledgements

Authors acknowledge the financial support received from Department of Electronics & Information Technology (MC & IT), Govt. of India to carry out the present study. The authors are also thankful to the Sophisticated Analytical Instrument Facility (SAIF), North-Eastern Hill University, Shillong and Central Instrumentation Facility, Indian Institute of Technology, Guwahati for providing TEM, SEM, and EDX facilities.

References

Ahmad, A., Mukherjee, P., Senapati, S., Mandal, D., Khan, M.I., Kumar, R., and Sastry, M. 2003. Extracellular biosynthesis of AgNPs using the fungus *Fusarium oxysporum*. *Coll. Surf. B: Biointerfaces* **28**, 313–318.

Bar, H., Bhui, D.K., Sahoo, G.P., Sarkar, P., De, S.P., and Misra, A. 2009. Green synthesis of AgNPs using latex of *Jatropha curcas*. *Coll. Surf. A.* **339**, 134–139.

Begum, N.A., Mondal, S., Basu, S., Laskar, R.A., and Mandal, D. 2009. Biogenic synthesis of Au and Ag nanoparticles using aqueous solutions of black tea leaf extract. *Coll. Surf. B: Biointerfaces* **71**, 113–118.

Bhagobaty, R.K. and Joshi, S.R. 2011. Metabolite profiling of endophytic fungal isolates of five ethno-pharmacologically important plants of Meghalaya, India. *J. Metabolomics. Syst. Biol.* **2**, 20–31.

Bhainsa, K.C. and D'Souza, S.K. 2006. Extracellular biosynthesis of AgNPs using the fungus *Aspergillus fumigates*. *Coll. Surf. B: Biointerfaces* **47**, 160–164.

Birla, S., Tiwari, V.V., Gade, A.K., Ingle, A.P., Yadav, A.P., and Rai, M.K. 2009. Fabrication of AgNPs by *Phoma glomerata* and its combined effect against *Escherichia coli*, *Pseudomonas aeruginosa* and *Staphylococcus aureus*. *Lett. Appl. Microbiol.* **48**, 173–179.

Cho, K.H., Park, J.E., Osaka, T., and Park, S.G. 2005. The study of antimicrobial activity and preservative effects of nanosilver ingredient. *Electrochim. Acta.* **51**, 956–960.

Dar, M.A., Ingle, A., and Rai, M. 2012. Enhanced antimicrobial acti-

vity of AgNPs synthesized by *Cryphonectria* sp. evaluated singly and in combination with antibiotics. *Nanomedicine* **9**, 105–110.

Devi, L.S., Bareh, D.A., and Joshi, S.R. 2013. Studies on biosynthesis of antimicrobial AgNPs using endophytic fungi isolated from the ethno-medicinal plant *Gloriosa superba* L. *Proc. Natl. Acad. Sci. India Sect. B Biol. Sci.* doi:10.1007/s40011-013-0185-7.

Devi, L.S. and Joshi, S.R. 2012. Antimicrobial and synergistic effects of AgNPs synthesized using soil fungi of high altitudes of Eastern Himalaya. *Mycobiology* **40**, 27–34.

Esumi, K., Tano, T., Suzuk, A., Torigoe, K., and Meguro, K. 1990. Preparation and characterization of bimetallic palladium-copper colloids by thermal decomposition of their acetate compound in organic solvent. *Chem. Mater.* **2**, 564–567.

Fayaz, A.M., Balaji, K., Girilal, M., Yadav, R., Kalaichelvan, P.T., and Venketesan, R. 2010. Biogenic synthesis of AgNPs and their synergistic effect with antibiotics: a study against Gram-positive and Gram-negative bacteria. *Nanomedicine* **6**, 103–109.

Fortin, D. and Beveridge, T.J. 2000. Mechanistic routes towards biomineral surface development, pp. 294. *In* Baeuerlein, E. (ed.), Biomineralisation: From Biology to Biotechnology and Medical Application. Wiley-VCH, Verlag, Germany.

Gade, A.K., Bonde, P., Ingle, A.P., Marcato, P.D., Durán, N., and Rai, M.K. 2008. Exploitation of *Aspergillus niger* for synthesis of AgNPs. *J. Biobased Mater. Bioenergy* **2**, 243–247.

Gade, A.K., Ingle, A., Whiteley, C., and Rai, M. 2010. Mycogenic metal nanoparticles: progress and applications. *Biotechnol. Lett.* **32**, 593–600.

Goia, D.V. and Matijevic, N. 1998. Preparation of monodispersed metal particles. *J. Chem.* **22**, 1203–1215.

Gong, P., Li, H., He, X., Wang, K., Hu, J., Zhang, S., and Yang, X. 2007. Preparation and antibacterial activity of Fe_3O_4@Ag nanoparticles. *Nanotechnology* **18**, 604–611.

Gordon, O., Vig Slenters, T., Brunetto, P.S., Villaruz, A.E., Sturdevant, D.E., Otto, M., Landmann, R., and Fromm, K.M. 2010. Silver coordination polymers for prevention of implant infection: thiol interaction, impact on respiratory chain enzymes, and hydroxyl radical induction. *Antimicrob. Agents Chemother.* **54**, 4208–4218.

Henglein, A. 2001. Reduction of $Ag(CN)_2$ on silver and platinum colloidal nanoparticles. *Langmuir* **7**, 2329–2333.

Huh, A.J. and Kwon, Y.J. 2011. "Nanoantibiotics": a new paradigm for treating infectious diseases using nanomaterials in the antibiotics resistant era. *J. Control. Release* **156**, 128–145.

Kim, S.H., Lee, H.S., Ryu, D.S., Choi, S.J., and Lee, D.S. 2011. Antibacterial activity of silver-nanoparticles against *Staphylococcus aureus* and *Escherichia coli. Kor. J. Microbiol. Biotechnol.* **39**, 77–85.

Kora, A.J. and Arunachalam, J. 2011. Assessment of antibacterial activity of AgNPs on *Pseudomonas aeruginosa* and its mechanism of action. *World J. Microbiol. Biotechnol.* **27**, 1209–1216.

Liu, X., Atwater, M., Wang, Q., and Huo, J. 2007. Extinction coefficient of gold nanoparticles with different sizes and different capping ligands. *Coll. Surf. B: Biointerfaces* **58**, 3–7.

Malabadi, R.B., Mulgund, G.S., Meti. N.T., Nataraja, K., and Kumar, S.V. 2012. Antibacterial activity of AgNPs synthesized by using whole plant extract of *Clitoria ternatea*. *Res. Pharm.* **2**, 10–21.

Mayr-Harting, A., Hedges, A., and Berkeley, R. 1972. Methods for studying bactericides, pp. 74. Academic Press, New York, N.Y., USA.

Mukherjee, P., Ahmad, A., Mandal, D., Senapati, S., Sainkar, S.R., Khan, M.I., Parischa, R., Ajayakumar, P.V., Alam, M., Kumar, R., and *et al.* 2001. Fungus-mediated synthesis of AgNPs and their immobilization in the mycelial matrix: A novel biological approach to nanoparticle synthesis. *Nano. Lett.* **1**, 515–519.

Musarrat, J., Dwivedi, S., Singh, B.J., Al-Khedhairy, A.A., Azam, A., and Naqvi, A. 2010. Production of antimicrobial AgNPs in water extracts of the fungus *Amylomyces rouxii* strain KSU-09. *Bioresour. Technol.* **101**, 8772–8776.

Nalwade, A.R., Shinde, S.S., Bhor, G.L., Admuthe, N.B., Shinde, S.D., and Gawade, V.V. 2013. Rapid biosynthesis of AgNPs using bottle gourd fruit extract and potential application as bactericide. *Res. Pharma.* **3**, 22–28.

Owen, N.L. and Hundley, N. 2004. Endophytes – the chemical synthesizers inside plants. *Sci. Prog.* **87**, 79–99.

Panacek, A., Kvitek, L., Prucek, R., Kolar, M., Vecerova, R., and Pizurova, N. 2006. Silver colloid nanoparticles: synthesis, characterization, and their antibacterial activity. *J. Phys. Chem. B* **110**, 16248–16253.

Pastoriza-Santos, L. and Liz-Marzan, M. 2002. Formation of PVP-protected metal nanoparticles in DMF. *Langmuir* **18**, 2888–2893.

Qian, Y., Yu, H., He, D., Yang, H., Wang, W., Wan, X., and Wang, L. 2013. Biosynthesis of AgNPs by the endophytic fungus *Epicoccum nigrum* and their activity against pathogenic fungi. *Bioprocess Biosyst. Eng.* **36**, 1613–1619.

Rai, M., Yadav, A., and Gade, A. 2009. AgNPs as a new generation of antimicrobials. *Biotechnol. Adv.* **27**, 76–83.

Rodriquez-Sanchez, L., Blanco, M.C., and Lopez-Quintela, M.A. 2000. Electrochemical synthesis of AgNPs. *J. Phys. Chem. B* **104**, 9683–9688.

Singh, M., Sing, S., Prasad, S., and Gambhir, I.S. 2008. Nanotechnology in medicine and antibacterial effect of silver nanoparticles. *Dig. J. Nanomater. Bios.* **3**, 115–122.

Sondi, I. and Salopel-sondi, B. 2004. AgNPs as antimicrobial agent: a case study on *E. coli* as a model for Gram-negative bacteria. *J. Coll. Interface Sci.* **275**, 177–182.

Song, J.Y. and Kim, B.S. 2009. Rapid biological synthesis of AgNPs using plant leaf extract. *Bioprocess Biosyst. Eng.* **32**, 79–84.

Strobel, G.A. 2003. Endophytes as sources of bioactive products. *Microb. Infect.* **5**, 535–544.

Strobel, G. and Daisy, B. 2003. Bioprospecting for microbial endophytes and their natural products. *Microbiol. Mol. Biol. Rev.* **67**, 491–502.

Strobel, G., Yang, X., Sears, J., Kramer, R., Sidhu, R.S., and Hess, W.M. 1996. Taxol from *Pestalotiopsis microspora*, an endophytic fungus of *Taxus wallachiana*. *Microbiology* **142**, 435–440.

Taleb, A., Petit, C., and Pileni, M.P. 1997. Synthesis of highly monodisperse AgNPs from AOT reverse micelles: a way to 2D and 3D self organization. *Chem. Mater.* **9**, 950–959.

Tan, R.X. and Zou, W.X. 2001. Endophytes: a rich source of functional metabolites. *Nat. Prod. Rep.* **18**, 448–459.

Vaidyanathan, R., Kalishwaralal, K., Gopalram, S., and Gurunathan, S. 2009. Nanosilver – The burgeoning therapeutic molecule and its green synthesis. *Biotechnol. Adv.* **27**, 924–937.

Verma, V.C., Kharwar, R.N., and Gange, A.C. 2010. Biosynthesis of antimicrobial AgNPs by the endophytic fungus *Aspergillus clavatus*. *Nanomedicine (Lond)* **5**, 33–40.

White, T., Bruns, T., Lee, S., and Taylor, J. 1990. PCR Protocols, pp. 315–322. *In* Innis, M.A., Gelfand, D.H., Shinsky, J.J., and White, T.J. (ed.), A Guide to Methods and Applications. Academic Press, San Diego, USA.

Wiley, B.J., Im, S.H., Li, Z.Y., McLellan, J., Siekkinen, A., and Xia, Y. 2006. Manoeuvring the surface plasmon resonance of silver nanostructures through shape-controlled synthesis. *J. Phys. Chem. B* **110**, 15666–15675.

Zhu, J.J., Liu, S.W., Palchik, O., Koltypin, Y., and Gedanken, A. 2000. Shape-controlled synthesis of AgNPs by pulse sonoelctrochemical method. *Langmuir* **16**, 6396–6399.